Title:

Microbiological and Rheological Dynamics of Mixed Biofilms formed by Bacteria and Eukaryotic Virus

Authors: Jing Gao[1,2], Clémence Abriat[1], Magdalena Laekas-Hameder[1], Nick Virgilio[3], Charles M. Dozois[2,4,] Caroline Quach[1,5], Marie-Claude Heuzey[3], Guy Lemay[1] and France Daigle[1,2 *]

1. Department of Microbiology, Infectious Diseases and Immunology, Université de Montréal, Montreal, Québec, Canada
2. CRIPA, Swine and Poultry Infectious Diseases Research Center, Faculty of Veterinary Medicine, University of Montreal, St-Hyacinthe, Québec, Canada.
3. CREPEC, Department of Chemical Engineering, Polytechnique Montréal, Montréal, Québec Canada.
4. Centre Armand-Frappier Santé Biotechnologie, Institut National de la Recherche Scientifique (INRS), Laval, Québec, Canada
5. Department of Pediatrics, Université de Montréal, Montreal, Québec, Canada

* Corresponding author: france.daigle@umontreal.ca ORCID: 0000-0001-6847-4729

Key words: biofilm, reovirus, bulk rheology, bacteria, *Escherichia coli*, virus-bacteria

Abstract

Biofilms are structured microbial communities embedded within an extracellular matrix that confers protection against environmental stresses. In both natural and clinical settings, biofilms are rarely composed of a single species and may also involve interactions with bacteriophages or even eukaryotic viruses. Since both biofilms and viruses are ubiquitous, and viruses remain among the neglected components of the microbiome, understanding their interactions is essential. In hospitalized patients, catheter colonization by biofilms markedly increases the risk of bacteremia and septicemia, and biofilm formation is almost inevitable during long-term catheterization. In this study, we investigated biofilm-forming capacities of uropathogenic *Escherichia coli* (UPEC) and clinical strains associated with catheter-related systemic infections. Selected strains were further examined to evaluate the influence of the ubiquitous mammalian reovirus on bacterial biofilm formation and to evaluate biofilm entrapment of viral particles and its impact on viral infectivity. Bacterial growth, survival and biofilm production were measured in the presence or absence of the virus. While reovirus exhibited no bactericidal effects and biofilm biomass remained largely unchanged, rheological and microscopic analyses revealed strain-specific alterations in biofilm properties. Remarkably, reovirus retains infectivity after release from biofilms, indicating that bacterial biofilms may serve as reservoirs or shelters for eukaryotic viruses.

Introduction

Most microorganisms naturally exist within biofilms, including when they are grown on the surface of a living organism, forming what are called host-associated biofilms. [1,2]. Biofilms are organized communities of microorganisms that adhere to surfaces and are embedded in a self-produced, mechanically robust, and protective polymeric extracellular substances (EPS) matrix. Biofilms are ubiquitous in nature and play important roles in various engineering

applications, including biocatalysis, microbial fuel cells, and bioreactors for wastewater treatment. However, biofilms are also implicated in biofouling, contamination, and infections. Clinical biofilms can enhance microbial persistence and resistance by up to 1000-fold [3], leading to higher costs, therapy failures, and, ultimately, patient mortality. Infections caused by biofilms on indwelling medical devices, such as prostheses and catheters, are a significant public health challenge and economic burden. It is therefore not surprising that the most common nosocomial infections are due to biofilms formed on medical devices [4]. Among these, catheter-associated urinary tract infections (CA-UTIs) [5] and central line-associated bloodstream infections (CLABSI) occur frequently [6]. Once a catheter is introduced *in situ*, from the external environment into the internal host environment, whether in the urinary tract or vascular system, microorganisms begin to invade and colonize both the host and the device, eventually leading to biofilm formation [7-9]. Uropathogenic *Escherichia coli* (UPEC) strains alone are responsible for 80 to 90% of UTI cases [10]. In contrast, nearly 64% of pathogens responsible for CLABSI are Gram-positive bacteria, with *Staphylococcus aureus* and coagulase-negative *Staphylococcus* spp. and *Enterobacter* spp. being the most frequently identified species [6].

Biofilms are rarely composed of a single bacterial species. Instead, the microbial community typically includes multiple species, often spanning different taxonomic kingdoms, such as viruses, protozoa, and fungi [1112]. In humans, mixed-species biofilms are found in various environments, including the oral cavity, chronic wounds, the intestinal tract, the lungs of cystic fibrosis patients, and on medical devices [13,14]. Although mixed-species biofilms appear to be the dominant form in nature, most research to date has focused on single-species biofilms. It is therefore essential to better understand the structure, physiology, communication mechanisms, and individual roles of each microorganism within polymicrobial biofilms.

Biofilm alteration during formation or maturation can be driven by multiple factors, such as environmental stressors, nutrient availability, oxygen levels, pH,

temperature, antimicrobial exposure, and biotic interactions [15-17]. Structural modifications may occur in multispecies biofilm, where different microorganisms coexist within a shared EPS matrix and display complex spatial organization. Multispecies interactions can result in competition for resources or, conversly, to metabolic cooperation, both of which can drive changes in biofilm architecture. These interactions may lead to increased cell density to enhance survival, as observed in dental plaque, antibiotic-resistant communities, or chronic infections [18-20], which promote structural remodeling that lead to detachment and dispersal.

Numerous studies have demonstrated that interactions with bacterial viruses (bacteriophages) can profoundly affect bacterial biofilms [21,22]. Bacteriophages can disrupt and eradicate biofilms by producing polymerases that degrade the EPS matrix or endolysins that lyse bacterial cells. Physical disturbance by phages can reduce biofilm biomass and weaken the overall community, highlighting their strong potential for biofilm dispersion [23]. At the opposite, some phage pressure can select for bacterial mutants with altered surface receptors (to avoid infection) that can lead to a hyper-biofilm phenotype that is both resistant to phages and more robust than the original biofilm. Further, some phages (often prophages) actively stabilize and promote biofilm growth [21,22,24]. In contrast, very little is currently known about the interactions between eukaryotic viruses and bacterial biofilms.

Thus, there is a growing need for novel approaches to study interactions between bacteria and mammalian viruses, as little research has addressed the influence of viral particles on biofilm development and behavior. Viruses, being ubiquitous and often co-located with bacteria, can become incorporated into biofilms. Within the biofilm matrix, they are protected from environmental stress, which may enhance their resistance and infectivity [25-28]. This coexistence presents a potential health risk. It is likely that numerous interactions between viruses and bacteria occur within the context of biofilms, and that biofilms may act as reservoirs for viruses. This would allow viral particles to persist in the host or environment,

remain infectious, and be shielded from desiccation, immune responses, and chemical treatments, among other stressors [26,27]. However, very limited information is available on the role or fate of mammalian viruses within microbial biofilms. Moreover, although viruses are recognized members of the urinary tract microbiome (urobiome) [29,30] or the skin microbiome [31,32] very few metagenomic studies have include the identification and analysis of eukaryotic viruses (the virome) associated with catheters. Mammalian reovirus is a ubiquitous, non-enveloped, double-stranded RNA virus that infects eukaryotic mammalian cells with a large host range and tissue tropism. It has been selected as a model eukaryotic virus for studying virus-bacteria interactions, as it can interact with planktonic bacteria and their envelope components, such as lipopolysaccharides (LPS) and peptidoglycan (PG), which is known to enhance viral thermostability within the host [33].

Various qualitative and quantitative approaches were used to characterize biofilm, such as crystal violet for total biomass, microscopy for architecture and rheology for matrix properties. Rheology, a technique used in materials science and engineering, measures the mechanical and viscoelastic properties of fluids and soft solids, like gels. More recently, it has been adapted to monitor biofilm formation and to assess the robustness of bacterial biofilms by quantifying their viscoelastic properties [34-36]. In these studies, the viscoelastic properties of single-species biofilms were compared with those of multispecies biofilms. Rheology is now considered an integral approach, alongside genetic analysis and matrix composition studies, for characterizing biofilm properties [37,38]. We hypothesize that viruses and bacteria interact directly within biofilms, influencing each other's persistence and possibly contributing to biofilm resilience, composition, and pathogenicity.

In this work, we evaluated the formation and properties of biofilms produced by bacterial clinical strain of UPEC and CLABSI (systemic) strains. Biofilm-forming strains from each group were selected for further analysis, including biofilm

formation in co-culture with or without reovirus infectious particles. Rheology was used to assess whether the virus affected the viscoelastic properties of the biofilm, while microscopy was employed to observe the spatial localization of the virus within the biofilm. Finally, the infectivity of the viral particles recovered from biofilm was determined. Overall, we concluded that viruses can persist within biofilms and can modulate biofilm properties in a strain-specific manner.

Results

Biofilm Formation. A collection of 14 uropathogenic *Escherichia coli* (UPEC) strains and 22 strains isolated from patients with catheter-associated infections, hereafter referred to as systemic strains (Table 1), were tested for their biofilm-forming capacities (Figure 1). Strain AR3110, an *E. coli* K-12 laboratory strain known to produce biofilms, was used as a positive control for *E. coli* strains [39]. The collection of systemic strains included eight *Staphylococcus epidermidis*, seven *Staphylococcus aureus*, two *Klebsiella oxycota*, two *Enterococcus faecalis*, one *E. coli*, one *Klebsiella pneumoniae*, and one *Staphylococcus capitis*. Biofilm biomass for the different strains was quantified using the standard crystal violet assay. Considerable variation in biomass production was observed among UPEC and systemic strains, as well as within individual species (Figure 1).

Four UPEC strains, U247, V11, Pyelo76, and JJ719 were selected based on their strong biofilm-forming ability. Strain CFT073 was selected as a prototypical model organism in studies of UPEC-associated urinary tract infections [40]. Systemic strains *K. oxytoca* (2), *S. capitis* (9), *S. aureus* (15b) and *S. epidermidis* (21) were chosen for further investigation into polymicrobial biofilms composed of bacteria and viruses. These strains were selected to investigate distinct species within biofilms in LB medium after 48 h of incubation at 37 °C.

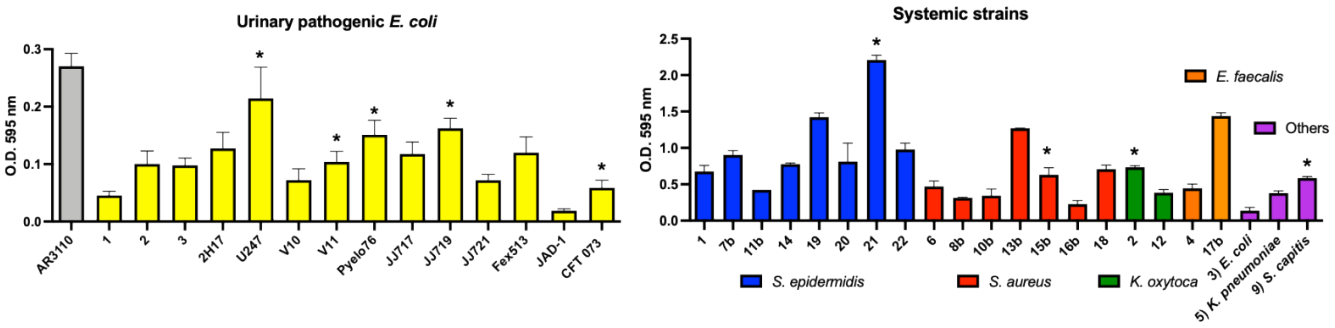

Figure 1. Biofilm biomass. Biomass formation by the UPEC strains and systemic strains was measured after 48 h at 37°C. Total biofilm biomass was quantified by measuring the OD_{595} of crystal violet-stained biofilms. Data are presented as mean ± standard error of the mean (SEM) from at least three independent biological replicates, each performed in duplicate. Asterisks (*) indicate strains selected for further characterization. The strain descriptions are summarized in Table 1.

Polymicrobial Interaction during Planktonic Growth. In order to characterize polymicrobial biofilms, growth and survival of the selected strains were evaluated with and without the presence of infectious viral particles. Since viruses were released from host cells using freeze-thaw cycles, lysate from non-infected host cells was used as a negative control. Bacteria were inoculated at a concentration of 10^3 bacteria/mL, either alone (bacteria), with infected cell lysate containing 10^7 infectious viral particles (plaque-forming units or pfu) per mL (bacteria + virus) or the same volume of uninfected cell lysates (Bacteria + uninfected cells). Growth curves of the selected UPEC strains are shown in Figure 2A. No significant growth defects were observed in any of the strains, and inclusion of uninfected or infected cell lysates even slightly enhanced bacterial growth. Since growth curves are based on optical density measurements, we also evaluated the number of viable bacterial cells after 20 h (Figure 2B). Again, the addition of either cell lysate did not affect

bacterial viability except for strain CFT073 that had a lower number of viable bacterial cells in the presence of the uninfected control cell lysate.

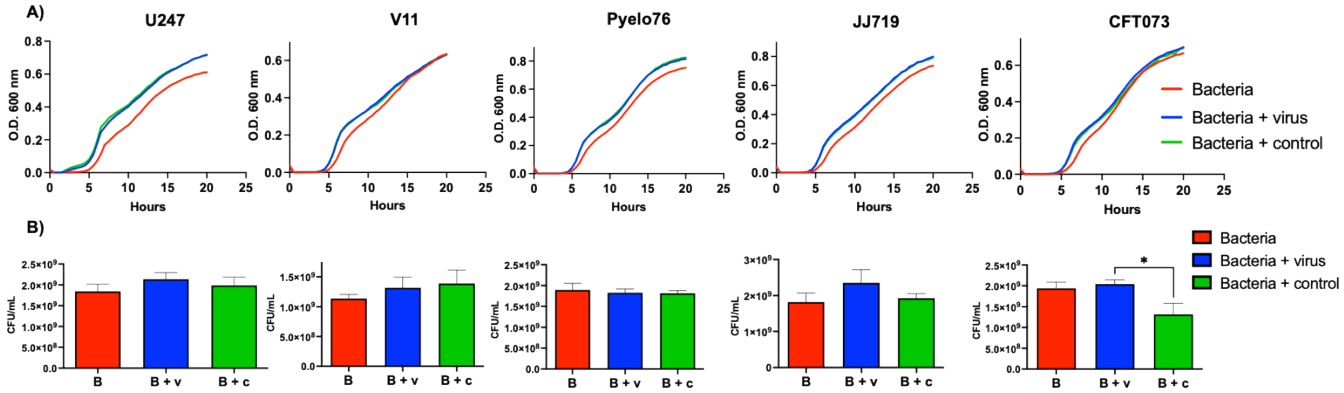

Figure 2. Planktonic growth and survival of UPEC strains.
A) The growth kinetics of selected UPEC strains grown alone (Bacteria; B; in red), in presence of infected cell lysate with virus (Bacteria + virus; B + v; in blue) or in presence of cell lysate from uninfected cells (Bacteria + control; B + c; in green) was measured by optical density for 20 h. B) Viable count of bacteria was determined by colony-forming units (cfu)/mL. Data are presented as mean ± standard error of the mean (SEM) from at least three independent biological replicates, each performed in duplicate. * Indicates a statistically significant difference determined by Student's t-test ($P < 0.05$).

Similarly, growth curves and viability of the systemic strains were evaluated and are shown in Figure 3. No significant growth defects were observed in any of the strains in the presence of either infected cell lysate containing viral particles or the control uninfected cell lysate (Figure 3A), and viability was not significantly affected either (Figure 3B). Overall, the addition of cell lysate, even if it contained infectious viral particles, neither impaired nor enhanced the growth or viability of the selected UPEC and systemic strains in planktonic conditions, nor did it induce

toxicity. These results provided a foundation to investigate the role of the virus in biofilm formation.

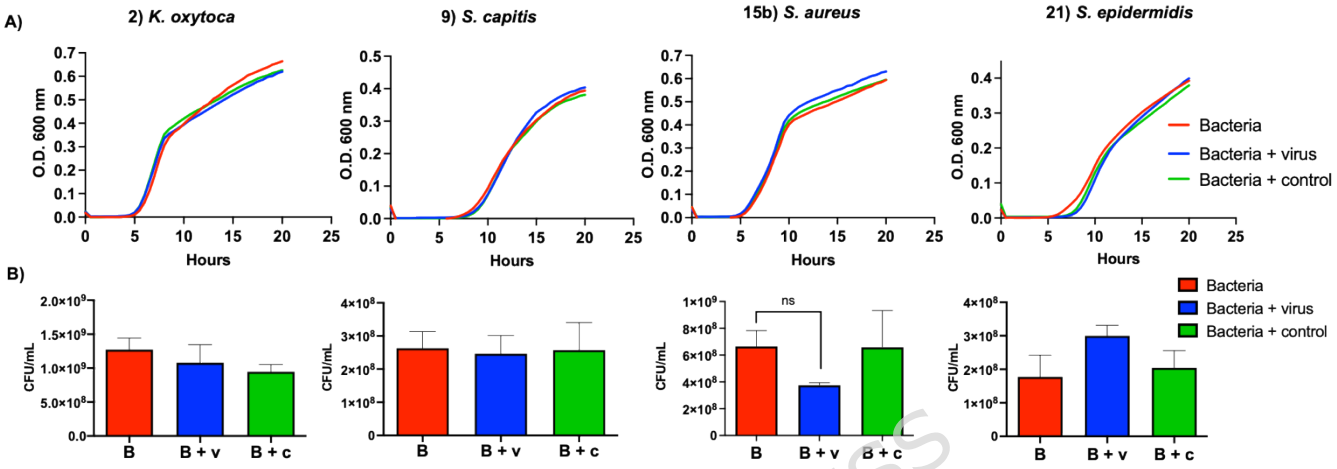

Figure 3. Planktonic growth and survival of systemic strains. A) Growth kinetics of selected systemic strains grown alone (Bacteria; B; in red), in presence of infected cell lysate with virus (Bacteria + virus; B + v; in blue) or in presence of cell lysates from uninfected cells (Bacteria + control; B + c; in green) was measured by optical density for 20 h. B) Viable counts of bacteria were determined by cfu/mL. Data are presented as mean ± standard error of the mean (SEM) from at least three independent biological replicates, each performed in duplicate. * Indicates a statistically significant difference determined by Student's t-test ($P < 0.05$).

Polymicrobial Biofilm. Biofilm formation in presence or absence of viral particles was evaluated using the crystal violet assay. Among the UPEC strains, only strain V11 was affected, showing reduced biofilm biomass upon the addition of either control lysate from uninfected cells or virus-containing cell lysates from infected cells. In systemic strains, the addition of either cell lysate increased biomass of *S. aureus* strain 15b biofilms, whereas both conditions reduced biomass of *S. epidermidis* strain 21 biofilms.

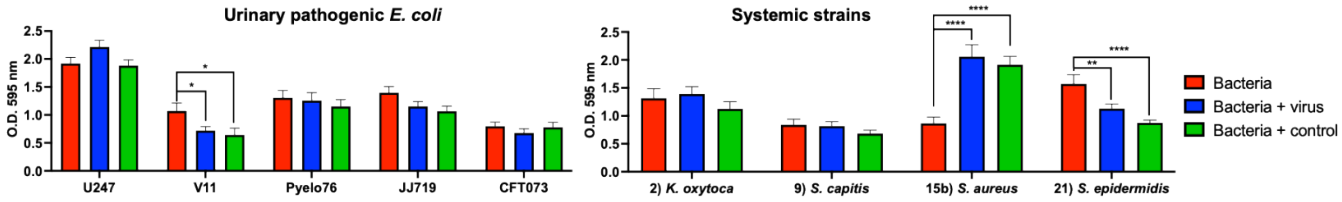

Figure 4. Biomass of polymicrobial biofilms. Biomass formation by the UPEC strains and systemic strains in presence and absence of viruses or uninfected cell lysate (control) was measured after 48 h at 37°C. Total biofilm biomass was quantified by measuring the OD_{595} of crystal violet-stained biofilms. Data are presented as mean ± standard error of the mean (SEM) from at least three independent biological replicates, each performed in duplicate. * Indicates a statistically significant difference determined by Student's t-test ****= $P < 0.001$, **= $P < 0.01$ *= $P < 0.05$.

Polymicrobial Biofilm Viscoelastic Properties. Since the presence of the virus did not affect planktonic bacterial growth, survival, or biofilm biomass, we proceeded to evaluate the rheological properties of the various biofilms in the absence of virus. To assess the mechanical properties of biofilms, bulk rheology was performed on mature biofilms (48 h) formed by the different bacterial strains. Oscillatory shear measurements were conducted to determine the storage modulus (G') and loss modulus (G''), which respectively reflect the elastic (solid-like) and viscous (liquid-like) behavior of the biofilm matrix. For each strain, frequency sweep tests (0.1–10 rad/s) were conducted within the linear viscoelastic region (Figure 5). The data quality across all replicates was consistent, with minimal variability between technical and biological replicates, allowing for robust comparative analysis.

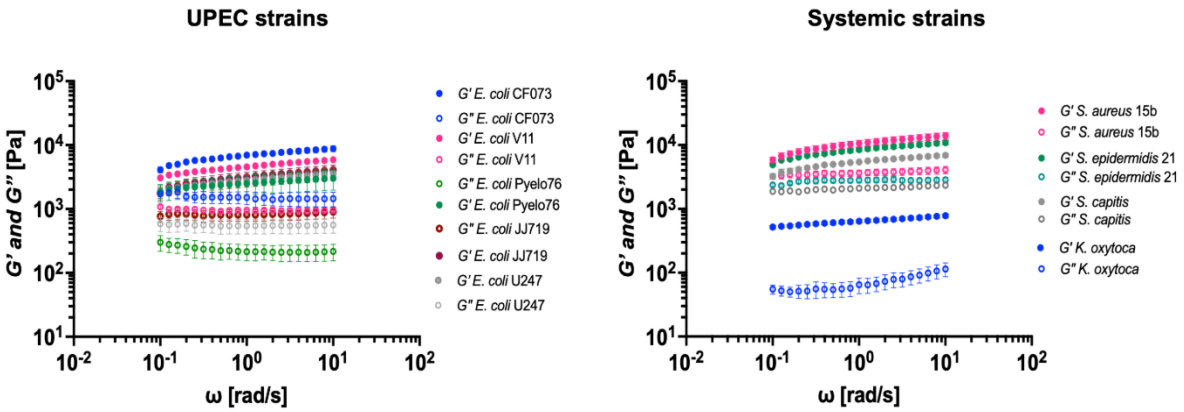

Figure 5. Bulk rheology of bacterial biofilm. Storage modulus (*G'*) and loss modulus (*G''*) were measured using oscillatory shear rheology to characterize the viscoelastic properties of the biofilm. *G´* represents the elastic, solid-like behavior of the biofilm, while *G˝* reflects its viscous, liquid-like response. Data are presented as the mean ± standard error of the mean (SEM) from at least three independent biological replicates done in duplicate.

All the strains exhibited a strong solid-like behavior, with *G´* much higher than *G˝* and no dependance on the frequency. However, biofilms displayed distinctive rheological properties, with *Klebsiella oxytoca* having a lower *G'* value for example. This being established, we then assessed the impact of viral presence on the biofilms. Biofilms of the selected strains were grown under three conditions: (i) alone**,** (ii) with virus-containing cell lysate or **(**iii) with control cell lysate**.**

For the UPEC strains, no significant differences in *G´* values were observed after the addition of virus to biofilm for most of the strains, except for U247 (Figure 6).

Interestingly, for this strain, the *G´* values were significantly increased in the presence of virus, compared to bacteria alone or the control cell lysate, suggesting enhanced biofilm stiffness or matrix crosslinking that was specific to the addition of virus. In contrast, the addition of virus is associated with a decrease in *G´* in strain CFT073, but the differences were not statistically significant. Regarding the systemic strains, most of the strains did not show significant differences in the *G´* values after biofilm formation in the presence or absence of virus, except for *S. epidermidis* (Figure 6). For this strain, the *G´* values were lower in the presence of virus compared to bacteria alone or control cell lysate, which was indicative of a weakened or more compliant matrix structure. Overall, bulk rheology showed that cell lysate exposure alters the mechanical integrity of bacterial biofilms, with virus presence exerting strain-dependent effects. The storage modulus (*G'*) proved to be a sensitive and quantitative indicator of biofilm structural dynamics.

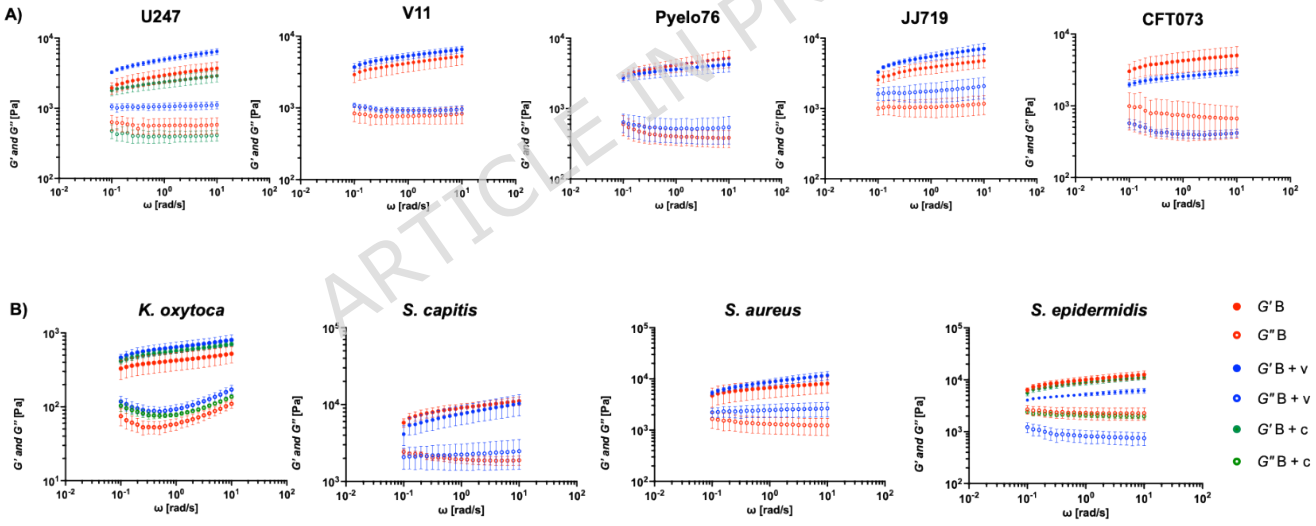

Figure 6. Bulk rheology of microbial biofilms, grown alone, or in the presence of infected or uninfected cell lysate. Storage modulus (*G'*) and loss modulus (*G˝*) were measured using oscillatory shear rheology to characterize the viscoelastic properties of the biofilm composed of bacteria alone, (B for bacteria) in presence of viruses (B + v) or

uninfected cell lysate (control)(B +c). A) UPEC strains and B) systemic strains. Data are presented as the mean ± standard error of the mean (SEM) from at least three independent biological replicates.

Localization of Virus within Polymicrobial Biofilms by Fluorescence Microscopy.

To assess the presence, spatial localization, and specificity of viruses within the biofilm, bacteria were incubated for 48 h with fluorescently labeled viral particles prepared from purified stocks, as described in Materials and Methods, or with fluorescent latex beads of similar size, followed by DAPI staining of the biofilms. DAPI staining revealed the overall biofilm morphology and bacterial cell organization, while the green fluorescent signal indicated the location of viral particles, and the red fluorescent signal corresponded to the beads. The two bacterial strains that exhibited opposite effects in bulk rheology, U247, which presented a higher *G'* in the presence of virus, and *S. epidermidis,* which showed a lower *G',* were further examined. Distinct fluorescent puncta corresponding to viral particles were detected throughout the biofilm, with signal intensity varying according to the depth and density of the matrix. Viral signal co-localized with dense microcolonies in both UPEC and systemic strains, suggesting preferential accumulation in specific microenvironments and association with bacterial networks. In contrast, latex beads were mostly observed in regions with sparse bacterial density (Figure 7). These results demonstrate that viral particles, unlike inert beads, can infiltrate and become embedded within bacterial biofilm matrices.

In addition to particle distribution, the presence of viral particles also seem to influence biofilm morphology in a strain-dependent manner, as observed by microscopy. For strain U247, addition of virus shifted the biofilms from aggregated clusters to a more sinusoidal, network-like structure (Figure 7A, compare in the

presence or absence of virus). Conversely, in *S. epidermidis*, the opposite effect was observed, leading to a transition from a network-like architecture to a more aggregated biofilm (Figure 7C).

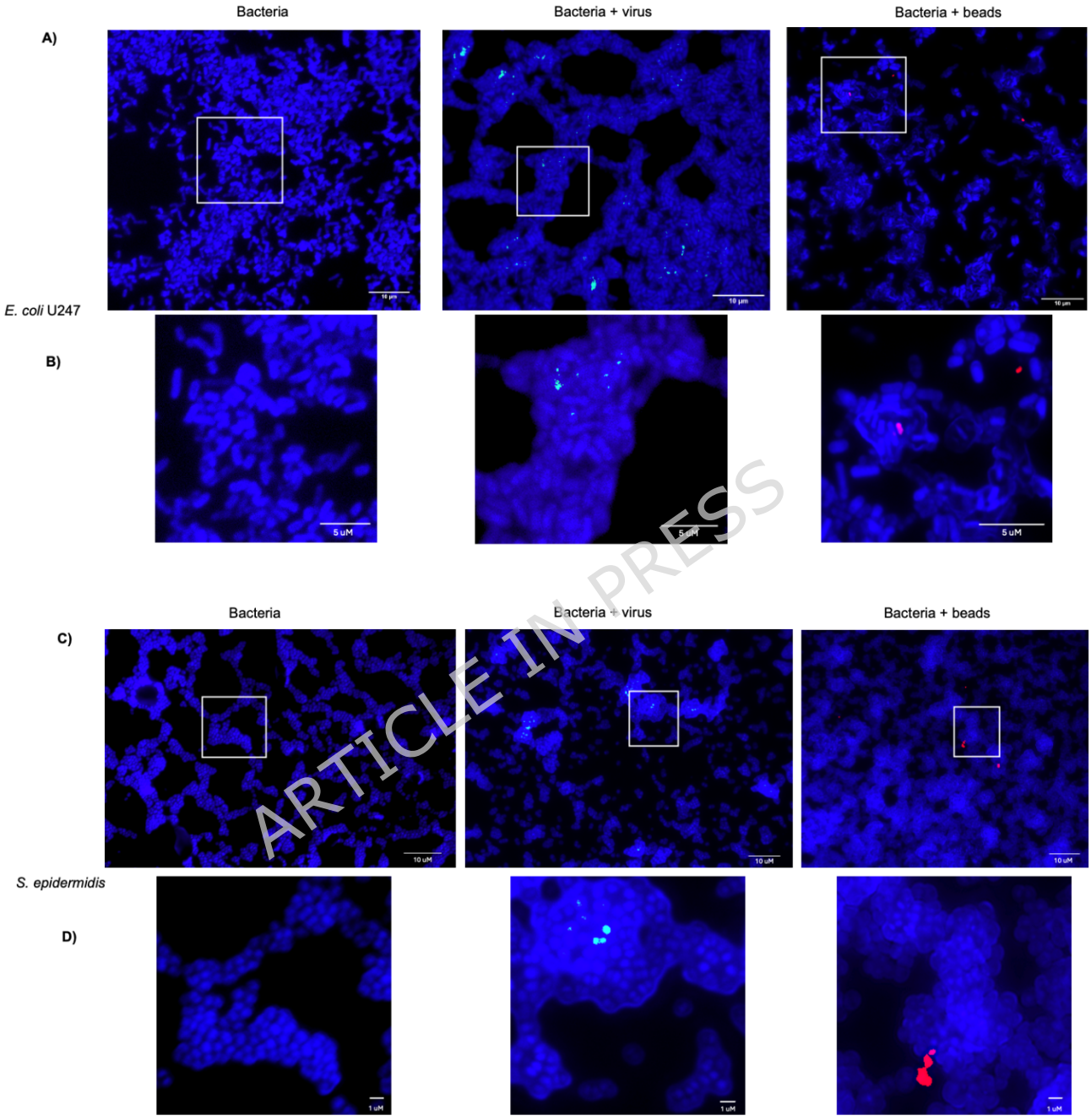

Figure 7. Fluorescence microscopy. Biofilm, alone or incubated with FITC-labeled viruses (green) or 0.1 mm red fluorescent latex beads for 48 h and stained with DAPI were visualized at 100X (scale bar, indicated on each image). Biofilm composed of A) UPEC strain U247, B) UPEC strain U247 with a magnified inset of an area of interest (white square) from A. C) systemic *S. epidermidis* strain 21, D) systemic *S. epidermidis* strain 21, with a magnified inset of an area of interest (white square) from C.

Virus Infectivity Following Biofilm Exposure

To investigate whether viral particles recovered from bacterial biofilms remain infectious and replication-competent, we used an engineered reovirus encoding NanoLuc luciferase upon infection**,** which provides a sensitive and quantitative readout of viral infectivity following recovery from biofilms. The luminescent virus was engineered, propagated and titered as described in Materials and Methods. This approach offers the added advantage of a short incubation period between the virus recovered from biofilm and the eukaryotic cell line used to assess viral infectivity, thus minimizing issues associated with bacterial contamination. Measured luciferase activity under the conditions used showed a good correlation with virus titer, as previously reported [41].

The luciferase-encoding virus was added to bacterial biofilms of strain U247 and *S. epidermidis* and incubated for 48 h. After incubation, viruses were recovered from the biofilm matrix by washing and mechanical disruption, followed by filtration to remove bacterial cells. The recovered virus was then used to infect fresh monolayers of L929 cells. Luminescence of infected cells was measured at 24 h post-infection. The same concentration of virus incubated in bacterial culture medium was used as the positive control. The strong luminescent signal obtained indicates that biofilm-trapped virus remains similarly infectious when sourced from either of the polymicrobial biofilms (Figure 8). Although the amount of recovered virus was low compared to the control sample, this could be mostly due to the difficulty of releasing the virus by mechanical disruption from the biofilm.

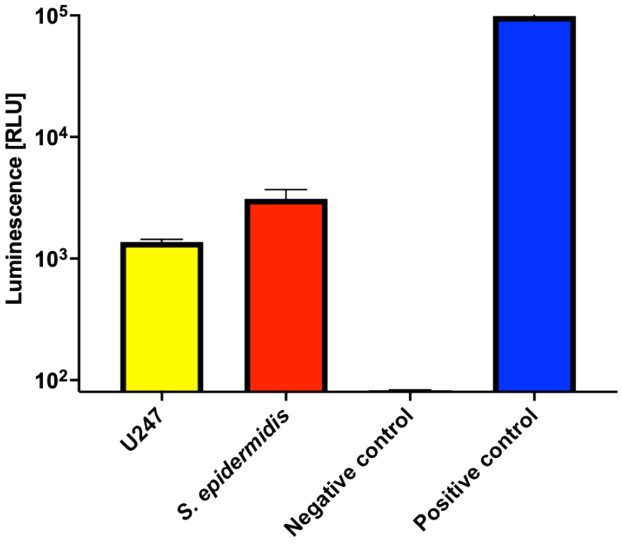

Figure 8. Luminescence of L929 cells infected with lysate obtained from polymicrobial biofilm composed of U247 or *S. epidermidis* and the luciferase-encoding reovirus. The virus incubated without bacteria was used as a positive control. Data represent the mean ± standard errors of the mean (SEM) of the results determined for 2 biological experiments in triplicate wells.

Discussion

Biofilms represent a major challenge in both clinical and environmental microbiology, as their complex architecture and protective extracellular matrix confer increased resistance to antimicrobials and host defenses. Although many studies have focused on single-species biofilms, natural biofilms are rarely comprised of a single strain or species. Instead, they often consist of polymicrobial communities in which interspecies interactions may influence colonization, persistence, and virulence. Because biofilms frequently form within indwelling devices, such as catheters, we investigated the biofilm-forming capacity of uropathogenic *Escherichia coli* (UPEC) strains, a major cause of catheter-

associated urinary tract infections as well as systemic strains isolated from patients with central line-associated infections. Selected biofilm-forming strains were further used to evaluate the impact of incorporating a eukaryotic virus within the biofilm, focusing on effects on biofilm biomass, architecture and viscoelastic properties, as well as on the stability of viral infectivity when viral particles are biofilm-associated.

Our collection of UPEC and systemic strains both demonstrated substantial variation in biofilm-forming capacity, ranging from weak to robust producers. This heterogeneity suggests that biofilm development is not a uniform trait within either group but rather a strain-dependent characteristic, suggesting that the ability to form biofilms is a highly variable trait across clinical isolates, rather than a defining feature of a specific pathotype. Such variability may reflect differences in genetic background, regulatory pathways, or adaptive responses to environmental conditions, with potential implications for virulence and persistence during infection.

Overall, the presence of infected cell lysate containing virus or control uninfected cell lysate had little to no effect on bacterial growth and survival (Figures 2, 3), with the exception of strain CFT073, which showed a modest survival defect when exposed to cell lysate. In contrast, biofilm biomass was more sensitive to these conditions, showing strain-dependent responses. While biomass was reduced in UPEC strain V11 and systemic strain *S. epidermis* 21, it was increased in *S. aureus* strain 15b (Figure 4). These findings suggest that interactions with virus or components of the cell lysate do not broadly impair bacterial proliferation but can differentially influence biofilm development in a strain- and species-specific manner. This variability may have important implications for understanding polymicrobial infections, where viral infection or virus-induced host cell damage could selectively hinder or promote biofilm development in different bacterial species.

Our rheological analyses demonstrate that bulk rheology is a robust and sensitive method to probe the physical properties of clinical biofilms, yielding reproducible strain-specific profiles (Figure 5). Importantly, the effects of virus addition (Figure 6) on biofilm mechanics also revealed the strain-dependent pattern observed in the biomass assays. For instance, the increase in the elastic modulus (G') of UPEC strain U247 suggests that viral components may promote a stiffer, more resilient biofilm matrix, whereas the reduced G' in *S. epidermidis* 21 indicates a weakening of structural integrity. Interestingly, in the case of these strains, components of the host cell lysate did not alter the mechanical properties of biofilms. When considered together, the biomass and rheological data reveal complementary dimensions of how the presence of virus can influence biofilms. It highlights that virus–bacteria interactions are not limited to altering the amount of biofilm formed, but can fundamentally reshape its mechanical resilience, which may have direct implications for persistence in host environments and resistance to clearance strategies.

Microscopy revealed that viruses were embedded within the biofilm, primarily associated with either the bacteria or the extracellular matrix (Figure 7). Notably, viral presence altered biofilm architecture in a strain-dependant manner, producing opposite morphological effects across the bacterial strains tested. These microscopic observations are consistent with the rheological data, which showed virus-dependent strengthening or weakening of the biofilm matrix (Figure 6). In contrast, sulfate-coated latex beads added to the bacterial biofilms showed minimal retention within the extracellular matrix compared to the viral particles, even at higher concentrations (Figure 7). Although the beads were similar in size to the viral particles, these inert spheres appeared to sediment more slowly and displayed no specific association with the biofilm. The lack of bead aggregates likely reflects their limited interaction and subsequent removal during washing, as they remained mostly suspended in the supernatant after 48 h of incubation.

Interestingly, viral infectivity can be retained after entrapment within the bacterial biofilm. It also showed that combined use of fluorescently-tagged virions and infectious virus encoding a luminescent reporter are powerful tools to track viruses in complex environments, such as polymicrobial biofilms or host interfaces. These findings further suggest that biofilms may serve as reservoirs for eukaryotic viruses. Beyond influencing biofilm production, biofilms can also affect viral stability. It was previously shown that biofilms can increase the stability of viruses [33,42]. In particular, the extracellular polymeric substances (EPS) produced within the biofilms play a key role in adenovirus persistence and stability [43].

The effect of a reovirus on biofilm biomass and mechanical properties was found to be strain-dependent, likely reflecting differences in bacterial physiology, such as adhesins, outer membrane proteins, or matrix composition. Viral particles may either reinforce the biofilm by becoming incorporated into the extracellular matrix or destabilize it, leading to reduced biomass. An indirect effect is also possible, whereby viral proteins or host-derived molecules provide additional nutrients or induce bacterial stress responses. Depending on the strain, such stress can upregulate biofilm-associated genes and increase biomass or conversely impair growth and promote detachment.

Although cohabitation between eukaryotic viruses and bacterial biofilms is now evident, it remains important to decipher the relationship and interplay between these microorganisms. An early study demonstrated that poliovirus particles could be associated with or become embedded within biofilm [26]. Similarly, the attachment of foodborne viruses to different surfaces was significantly increased by the presence of biofilm [44]. Co-infection with respiratory viruses, such as respiratory syncytial virus, rhinovirus, and adenovirus has been shown to increase the biofilm growth of *Pseudomonas aeruginosa* [45] and *Staphylococcus aureus* [46] on host epithelial cells. Moreover, even when *Pseudomonas* biofilm biomass remained

unchanged, co-infection with influenza virus significantly altered the host immune response [47].

The ability of viruses to associate with and persist within biofilms also raises the possibility that biofilms act as reservoirs for viral particles. By embedding within the biofilm matrix, viruses may be shielded from environmental stressors, host immune defenses, or antiviral treatments. This protective niche could prolong viral survival and facilitate subsequent release or transmission under favorable conditions. Such a role would not only complicate eradication strategies but could also contribute to recurrent or chronic infections in clinical and environmental settings.

Our findings demonstrate co-existence, persistence, and viability of viruses that are retained within and are potentially protected in a bacterial biofilm. This study does not demonstrate that the currently investigated biofilm interactions are directly associated with actual hospital infections in a clinical setting, but underline the potential likelihood of occurence of such mixed viral and bacterial associations within the context of biofilms in both clinical as well as other distinct ecological environments. It is therefore essential to deepen our understanding of the mechanisms governing polymicrobial biofilms, as they not only underlie persistent and recurrent infections but also complicate therapeutic outcomes. Unraveling the complex interactions between bacterial and viral partners within these communities will be critical for the development of innovative strategies aimed at prevention, disruption, and treatment. Such insights hold promise for improving patient outcomes and reducing the burden of biofilm-associated diseases.

Material and Methods

Bacterial Strains and Growth Conditions

Fourteen uropathogenic *Escherichia coli* (UPEC) strains from different sources and 22 clinical strains isolated from patients with catheter-associated infections at the Ste-Justine Hospital were included to investigate biofilms (Table 1). The clinical *E. coli* isolates consisted of previously well-characterized strains recovered from urine or blood cultures of patients diagnosed with extraintestinal infections. These isolates were obtained from the James Johnson collection [48,49], the Manges collection [50], the Dozois collection and the Institut Pasteur (Guadeloupe) collection [51]. The clinical systemic strains were obtained through the standardized and mandatory CLABSI provincial surveillance program (SPIN-BACC, INSPQ) and approved for used by the CHU Ste-Justine ethics board. All procedures were conducted in compliance with CHU institutional guidelines and regulations, and informed consent was obtained from the patient or their legal guardian. Bacteria were routinely cultured at 37°C in lysogeny broth (LB) (10 g/L tryptone, 5 g/L yeast extracts, and 10 g/L NaCl) (Bio Basic, Canada). For biofilm assays and rheology with UPEC strains, LB with no salt (LBNS) (10 g/L tryptone and 5 g/L yeast extracts) (Bio Basic, Canada)was used. For rheology with systemic strains, Trypticase Soy Broth and 1% glucose (TSBg) (Bio Basic, Canada)or with 1.5% agar (TSAg) (Wisent, Canada) was used.

Biofilm Quantification Assay

Bacteria from overnight cultures in LB broth were diluted to a final concentration of 10^3 CFU/mL in LB medium (for systemic strains) or LBNS (for UPEC strains) and transferred into 96-well plates (Sarstedt, Canada) and incubated statically at 37°C for 48 h. Following incubation, the supernatant was carefully aspirated from the bottom of each well to preserve the biofilm. Wells were washed once with non-sterile deionized water and air-dried for 20 min at 45°C. Biofilm biomass was quantified by crystal violet staining. Briefly, biofilms were incubated with 0.5% (w/v) crystal violet solution (Millipore- Sigma, USA) for 30 min at room temperature, after which excess dye was removed, and wells were washed three times with deionized water. Plates were air-dried, photographed, and examined

under an inverted microscope at 10× and 40× magnification. To quantify biofilm biomass, plates were destained with 30% acetic acid (Millipore- Sigma, USA), and the optical density of each well was measured at 595 nm using a SpectraMax® ABS Plus (Molecular Devices, USA) microplate reader. At least three biological replicates were performed for each strain, with technical duplicates. When indicated, 20 µL of viruses (10^8 PFU/mL) or cell lysate was added at the start of the assay, and biofilm formation was assessed as described above.

Cells and Viruses

Mouse L929 fibroblasts were originally obtained from the American Type Culture Collection (USA) (NTCC clone 929) and routinely maintained and propagated in MEM with 1% glutamine, 5% fetal bovine serum and antibiotics (Wisent, Canada). The Dearing strain of mammalian orthoreovirus was also originally obtained from the American Type Culture Collection. The viral stock of the laboratory was more recently sequenced and is referred to as T3D-Sandekian ($T3D^S$). The plasmids corresponding to the different $T3D^S$ genes for virus rescue by reverse genetics were previously reported [52].

Experimental viral stocks were prepared by infection of L929 cells without serum and antibiotics; infected cells and medium were then subjected to three cycles of freeze-thaw (-80°C to room temperature) 24 h post-infection before the determination of infectious titer by $TCID_{50}$, as previously described [53]. For negative control, cell lysate was similarly prepared in the absence of virus.

Growth Curves in the Presence of Virus

Bacteria were inoculated in LB broth and incubated for 20 h at 37°C with shaking. Cultures were diluted to a final concentration of 10^3 CFU/mL in LB medium (for systemic strains) or LBNS (for UPEC strains). Equal volumes of the bacterial suspension were dispensed in duplicate into the wells of 96-well plates (Sarstedt, Canada), as described for the biofilm quantification assay, alone or with 20 µL of infected cell lysate containing infectious virus (10^8 PFU/mL), or with 20 µL of

control uninfected cell lysate. Optical density at 600 nm was measured every 30 min over a 20 h incubation period at 37°C using a SpectraMax® iD3 Multi-Mode plate reader (Molecular Devices, USA). Each measurement was preceded by 3 seconds of shaking. For each bacterial strain, at least three independent biological replicates were performed, and results are presented as the mean ± standard error of the mean (SEM).

Bacterial Cell Viability in the Presence of Virus

To evaluate bacterial survival in the presence of virus, cultures were diluted to 10^3 CFU/mL, and incubated for 20 h at 37 °C under three conditions: bacteria alone, bacteria with 20 μL of infected cell lysate with virus (10^8 PFU/mL), or bacteria with 20 μL of control uninfected cell lysate. Serial 1:10 dilutions were prepared, colonies were counted the following day, and CFU/mL values were calculated. At least three biological replicates were performed for each selected bacterial strain and experimental condition.

Bulk Rheology

A rotational rheometer (TA Instruments Discovery, USA) was used for these experiments, with the temperature maintained at 37 °C using a Peltier plate. 300 μL of an overnight or a 10^4 dilution of bacterial culture of the selected UPEC or systemic strains were transferred onto a 0.4 μM polycarbonate (PC) filter (Millipore-Sigma, USA), placed on top of an agar plate and grown for 48 h. The filter harboring the colony biofilm was transferred to the rheometer to assess the viscoelastic properties of the biofilm in the bulk state. A 20 mm parallel plate with sand-paper was used for the oscillatory measurements. The gap was determined by lowering the plate until a normal force of 0.1N was detected, between 80 and 400 μm.

A frequency sweep was performed from 0.1 rad/s to 10 rad/s with a fixed deformation of 0.5%, followed by a deformation amplitude sweep from 0.1 to 200 % at 1 rad/s (Figure 9). The deformation amplitude sweep assay, a destructive test

in the case of these structures, determined the linear viscoelastic region (LVER) of the biofilm. This region defines the range of applied strain (or stress) where the mechanical properties (G' and G'') remain constant. Most biofilms showed a stable G' up to ~1% strain, after which G' declined, indicating matrix disruption (Figure 9). All subsequent frequency sweep measurements were performed within this LVER to ensure accurate, non-destructive characterization.

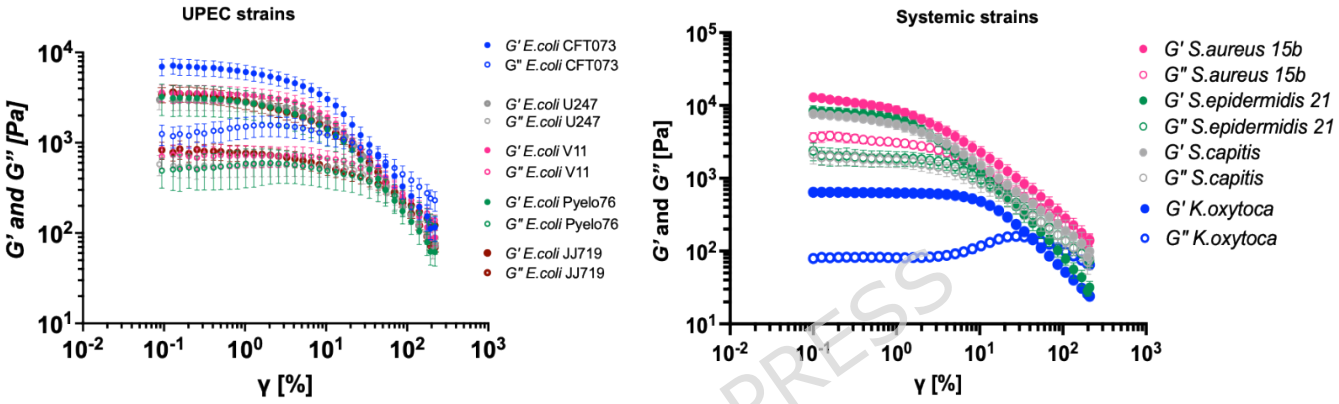

Figure 9. Deformation amplitude sweep assay performed on UPEC and systemic strains.

Preparation of Fluorescently Labeled Reovirus Virions

Virions were purified from infected cells by Vertrel (Enviro Tech, USA) extraction followed by ultracentrifugation on a cesium chloride gradient, using essentially standard procedures [54]. They were then fluorescently labeled using a standard procedure [55]. Briefly, potassium acetate buffer pH 9.5 was added at a final concentration of 50 mM to purified virions at approximately 1 mg/mL of virions. Fluorescein isothiocyanate (FITC)(Millipore-Sigma, USA) was then added to a final concentration of 1 mg/mL in a final reaction volume of 1 mL. The reaction was left to proceed for 1 h at room temperature in the dark. Unincorporated fluorochrome was then removed by dialysis against one liter of dialysis buffer (Tris-HCl 10 mM,

pH 7.5; NaCl 150 mM) for 48 h with buffer replacement after 24 h. Analysis on SDS-PAGE confirms the presence of fluorescently labeled viral proteins with the absence of free dye.

Fluorescence Microscopy

Overnight cultures were diluted to 10^3 CFU/mL in an 8-well cell culture chamber with a coverslip placed at the bottom (Sarstedt, Canada) with 10^7 virus particles or 10^7 or 10^8 fluorescent beads (Latex beads, sulfate-modified polystyrene, fluorescent red, aqueous suspension, 0.1 um) (Millipore-Sigma, USA) and incubated at 37°C for 48 h. After incubation, biofilms were gently washed to remove unbound particles and fixed in 2% glutaraldehyde in PBS, pH 7.4, for 15 min at room temperature. Coverslips were washed three times in PBS. Biofilms were then stained with DAPI (1:1000, Thermo Scientific, USA) for 15 minutes at room temperature. Fluorescence microscopy was then performed to evaluate particle distribution within the biofilm under a Nikon Eclipse Ti2 (Nikon, USA) fluorescent inverted microscope.

Recovery of Luciferase-Encoding Reovirus by Reverse Genetics

The plasmid encoding luciferase (Nano-Luc) in the σ3-encoding L1 gene of reovirus type 1 Lang (T1L) [41] was obtained from Addgene (USA) (plasmid #128942). Luciferase-encoding virus was rescued by plasmid-based reverse genetics, as previously described [56]. The nine viral genes, comprising the genetic background of the rescued virus, combined with the L1 gene encoding luciferase, were from $T3D^S$. The recovered virus was propagated in L929 cells in the absence of serum and antibiotics and titrated by $TCID_{50}$. When used to infect L929 cells, one $TCID_{50}$ unit was shown to result in approximately one luciferase unit 15-20 h post-infection (data not shown) using the assay described below.

Infectivity of Virus Recovered from Biofilms

Overnight cultures of UPEC and systemic strains were diluted and incubated with the virus for 1 h at 37 °C to allow the bacteria-virus attachment and then spotted onto a PC filter placed on agar plates, followed by an incubation of 48 h to allow colony biofilm development. Filters containing the colony biofilm were transferred into 1.5 mL microcentrifuge tubes with 300 µL PBS and subjected to two rounds of sonication (12 one-second pulses at 20 % amplitude) using a Vibra-cell sonicator (UltraSonics, USA), equipped with a micro-tip probe. The resulting suspension was filtered through a 0,22 µm to remove bacterial cells. 200 µL of the filtrate containing the viral suspension was used to infect L929 cells in a single well of a 12-well plate. After a one-hour adsorption period at 4 °C, 200 µL of antibiotic-containing medium was added, and cells were incubated at 37°C under a 5% CO_2 for 15 h before freezing at -80°C. Plates were thawed at room temperature, and 50 µL aliquots were used for luciferase activity according to the manufacturer's instructions (Promega). Luminescence was read using SpectraMax® iD3 Multi-Mode plate reader (Molecular Devices, USA).

Statistical analysis

All statistical analysis was performed using two-tailed unpaired parametric Student's *t*-test and the mean ± SEM is represented using the software GraphPad Prism 10.

Author contributions

JG performed the bacterial growth, survival and biofilms experiments. CA conducted the rheological analyses. MLH produced the virus stock and luminescent constructs. GL and MCH contributed to and data analysed and interpretation. CMD and CQ provided bacterial strains. NV, GL, CQ, MCH and FD secured funding. FD was the major contributor to manuscript writing. All authors read and approved the final version of the manuscript.

Acknowledgements

Funding

This work was supported by a grant NFRFE-2022-00464 from the New Frontiers in Research Fund and from the Swine and Poultry Infectious Diseases Research Center (CRIPA) funded by Fonds de recherche du Québec - Nature et technologies (FRQNT).

Additional information

All authors declare no financial or non-financial competing interests.

Data Availability

The datasets used and/or analyzed during the current study available from the corresponding author on request.

References

1 Flemming, H. C. *et al.* Biofilms: an emergent form of bacterial life. *Nat Rev Microbiol* **14**, 563-575, doi:10.1038/nrmicro.2016.94 (2016).

2 Costerton, J. W., Stewart, P. S. & Greenberg, E. P. Bacterial biofilms: a common cause of persistent infections. *Science* **284**, 1318-1322, doi:10.1126/science.284.5418.1318 (1999).

3 Hoyle, B. D. & Costerton, J. W. Bacterial resistance to antibiotics: the role of biofilms. *Prog Drug Res* **37**, 91-105, doi:10.1007/978-3-0348-7139-6_2 (1991).

4 Bryers, J. D. Medical biofilms. *Biotechnol Bioeng* **100**, 1-18, doi:10.1002/bit.21838 (2008).

5 Trautner, B. W. & Darouiche, R. O. Role of biofilm in catheter-associated urinary tract infection. *Am J Infect Control* **32**, 177-183, doi:10.1016/j.ajic.2003.08.005 (2004).

6 Gahlot, R., Nigam, C., Kumar, V., Yadav, G. & Anupurba, S. Catheter-related bloodstream infections. *Int J Crit Illn Inj Sci* **4**, 162-167, doi:10.4103/2229-5151.134184 (2014).

7 Azevedo, A. S., Almeida, C., Melo, L. F. & Azevedo, N. F. Impact of polymicrobial biofilms in catheter-associated urinary tract infections. *Crit Rev Microbiol* **43**, 423-439, doi:10.1080/1040841X.2016.1240656 (2017).

8 Wilks, S. A., Koerfer, V. V., Prieto, J. A., Fader, M. & Keevil, C. W. Biofilm Development on Urinary Catheters Promotes the Appearance of Viable but Nonculturable Bacteria. *mBio* **12**, doi:10.1128/mBio.03584-20 (2021).

9 Donlan, R. M. Biofilms: microbial life on surfaces. *Emerg Infect Dis* **8**, 881-890, doi:10.3201/eid0809.020063 (2002).

10 Flores-Mireles, A., Hreha, T. N. & Hunstad, D. A. Pathophysiology, Treatment, and Prevention of Catheter-Associated Urinary Tract Infection. *Top Spinal Cord Inj Rehabil* **25**, 228-240, doi:10.1310/sci2503-228 (2019).

11 Peters, B. M., Jabra-Rizk, M. A., O'May, G. A., Costerton, J. W. & Shirtliff, M. E. Polymicrobial interactions: impact on pathogenesis and human disease. *Clin Microbiol Rev* **25**, 193-213, doi:10.1128/CMR.00013-11 (2012).

12 Sadiq, F. A. *et al.* Trans-kingdom interactions in mixed biofilm communities. *FEMS Microbiol Rev* **46**, doi:10.1093/femsre/fuac024 (2022).

13 Elias, S. & Banin, E. Multi-species biofilms: living with friendly neighbors. *FEMS Microbiol Rev* **36**, 990-1004, doi:10.1111/j.1574-6976.2012.00325.x (2012).

14 Brogden, K. A., Guthmiller, J. M. & Taylor, C. E. Human polymicrobial infections. *Lancet* **365**, 253-255, doi:10.1016/S0140-6736(05)17745-9 (2005).

15 Kilic, T. in *Exploring bacterial biofilms* (ed InTech) (InTech, 2025).

16 Ugwu, C. *et al.* Biofilms: structure, resistance mechanism, emerging control strategies, and applications. *RCS Pharmaceutics* **6**, doi:DOI: 10.1039/D5PM00094G (2025).

17 Goller, C. C. & Romeo, T. Environmental influences on biofilm development. *Curr Top Microbiol Immunol* **322**, 37-66, doi:10.1007/978-3-540-75418-3_3 (2008).
18 Biswas, T., Ahmed, M. & Mondal, S. Mixed species biofilm: Structure, challenge and its intricate involvement in hospital associated infections. *Microb Pathog* **195**, 106866, doi:10.1016/j.micpath.2024.106866 (2024).
19 Joshi, R. V., Gunawan, C. & Mann, R. We Are One: Multispecies Metabolism of a Biofilm Consortium and Their Treatment Strategies. *Front Microbiol* **12**, 635432, doi:10.3389/fmicb.2021.635432 (2021).
20 Gordon, V., Bakhtiari, L. & Kovach, K. From molecules to multispecies ecosystems: the roles of structure in bacterial biofilms. *Phys Biol* **16**, 041001, doi:10.1088/1478-3975/ab1384 (2019).
21 Visnapuu, A., Van der Gucht, M., Wagemans, J. & Lavigne, R. Deconstructing the Phage-Bacterial Biofilm Interaction as a Basis to Establish New Antibiofilm Strategies. *Viruses* **14**, doi:10.3390/v14051057 (2022).
22 Sutherland, I. W., Hughes, K. A., Skillman, L. C. & Tait, K. The interaction of phage and biofilms. *FEMS Microbiol Lett* **232**, 1-6, doi:10.1016/S0378-1097(04)00041-2 (2004).
23 Chang, C. *et al.* Bacteriophage-Mediated Control of Biofilm: A Promising New Dawn for the Future. *Front Microbiol* **13**, 825828, doi:10.3389/fmicb.2022.825828 (2022).
24 Burkle, M. *et al.* Phage-phage competition and biofilms affect interactions between two virulent bacteriophages and *Pseudomonas aeruginosa*. *ISME J* **19**, doi:10.1093/ismejo/wraf065 (2025).
25 Wingender, J. & Flemming, H. C. Biofilms in drinking water and their role as reservoir for pathogens. *Int J Hyg Environ Health* **214**, 417-423, doi:10.1016/j.ijheh.2011.05.009 (2011).
26 Quignon, F., Sardin, M., Kiene, L. & Schwartzbrod, L. Poliovirus-1 inactivation and interaction with biofilm: a pilot-scale study. *Appl Environ Microbiol* **63**, 978-982, doi:10.1128/aem.63.3.978-982.1997 (1997).
27 Ascione, C. *et al.* Herpes simplex virus-1 entrapped in *Candida albicans* biofilm displays decreased sensitivity to antivirals and UVA1 laser treatment. *Ann Clin Microbiol Antimicrob* **16**, 72, doi:10.1186/s12941-017-0246-5 (2017).
28 Lacroix-Gueu, P., Briandet, R., Leveque-Fort, S., Bellon-Fontaine, M. N. & Fontaine-Aupart, M. P. In situ measurements of viral particles diffusion inside mucoid biofilms. *C R Biol* **328**, 1065-1072, doi:10.1016/j.crvi.2005.09.010 (2005).
29 Wojciuk, B. *et al.* Urobiome: In Sickness and in Health. *Microorganisms* **7**, doi:10.3390/microorganisms7110548 (2019).
30 Whiteside, S. A., Razvi, H., Dave, S., Reid, G. & Burton, J. P. The microbiome of the urinary tract--a role beyond infection. *Nat Rev Urol* **12**, 81-90, doi:10.1038/nrurol.2014.361 (2015).

31 Bjerre, R. D. *et al.* Skin dysbiosis in the microbiome in atopic dermatitis is site-specific and involves bacteria, fungus and virus. *BMC Microbiol* **21**, 256, doi:10.1186/s12866-021-02302-2 (2021).

32 Chen, Y. E. & Tsao, H. The skin microbiome: current perspectives and future challenges. *J Am Acad Dermatol* **69**, 143-155, doi:10.1016/j.jaad.2013.01.016 (2013).

33 Berger, A. K., Yi, H., Kearns, D. B. & Mainou, B. A. Bacteria and bacterial envelope components enhance mammalian reovirus thermostability. *PLoS Pathog* **13**, e1006768, doi:10.1371/journal.ppat.1006768 (2017).

34 Hollenbeck, E. C. *et al.* Molecular determinants of mechanical properties of *V. cholerae* biofilms at the air-liquid interface. *Biophys J* **107**, 2245-2252, doi:10.1016/j.bpj.2014.10.015 (2014).

35 Abriat, C. *et al.* Mechanical and microstructural insights of *Vibrio cholerae* and *Escherichia coli* dual-species biofilm at the air-liquid interface. *Colloids Surf B Biointerfaces* **188**, 110786, doi:10.1016/j.colsurfb.2020.110786 (2020).

36 Abriat, C., Virgilio, N., Heuzey, M. C. & Daigle, F. Microbiological and real-time mechanical analysis of *Bacillus licheniformis* and *Pseudomonas fluorescens* dual-species biofilm. *Microbiology (Reading)* **165**, 747-756, doi:10.1099/mic.0.000819 (2019).

37 Charlton, S. G. V. *et al.* Regulating, Measuring, and Modeling the Viscoelasticity of Bacterial Biofilms. *J Bacteriol* **201**, doi:10.1128/JB.00101-19 (2019).

38 Beckwith, J., K, Ganesan, M., VanEpps, J., S, Kumar, A. & Solomon, M., J. Rheology of *Candida albicans* fungal biofilms. *J. Rheol* **66**, 683-697 (2022).

39 Serra, D. O., Richter, A. M. & Hengge, R. Cellulose as an architectural element in spatially structured *Escherichia coli* biofilms. *J Bacteriol* **195**, 5540-5554, doi:10.1128/JB.00946-13 (2013).

40 Mobley, H. L. *et al.* Pyelonephritogenic *Escherichia coli* and killing of cultured human renal proximal tubular epithelial cells: role of hemolysin in some strains. *Infect Immun* **58**, 1281-1289, doi:10.1128/iai.58.5.1281-1289.1990 (1990).

41 Kanai, Y., Kawagishi, T., Matsuura, Y. & Kobayashi, T. In Vivo Live Imaging of Oncolytic Mammalian Orthoreovirus Expressing NanoLuc Luciferase in Tumor Xenograft Mice. *J Virol* **93**, doi:10.1128/JVI.00401-19 (2019).

42 Hassanbhai, A. M., Phoon, M. C., Chow, V. T. & Ho, B. The Association of *Helicobacter pylori* Biofilm with Enterovirus 71 Prolongs Viral Viability and Survival. *Int J Mol Sci* **24**, doi:10.3390/ijms241914500 (2023).

43 Greaves, J. C. *et al.* Extended persistence and thermostability of adenovirus 41 in the presence of bacteria. *J Appl Microbiol*, doi:10.1093/jambio/lxaf221 (2025).

44 Gagné, M. J., Savard, T. & Brassard, J. Interactions Between Infectious Foodborne Viruses and Bacterial Biofilms Formed on Different Food Contact Surfaces. *Food Environ Virol* **14**, 267-279, doi:10.1007/s12560-022-09534-z (2022).

45 Hendricks, M. R. *et al.* Respiratory syncytial virus infection enhances *Pseudomonas aeruginosa* biofilm growth through dysregulation of nutritional immunity. *Proc Natl Acad Sci U S A* **113**, 1642-1647, doi:10.1073/pnas.1516979113 (2016).
46 Kiedrowski, M. R. *et al. Staphylococcus aureus* Biofilm Growth on Cystic Fibrosis Airway Epithelial Cells Is Enhanced during Respiratory Syncytial Virus Coinfection. *mSphere* **3**, doi:10.1128/mSphere.00341-18 (2018).
47 Hall, J. *et al.* Effects of influenza A infection on liberation of bacteria from biofilms and inflammatory response in an in vitro model of chronic rhinosinusitis. *Microbiology (Reading)* **171**, doi:10.1099/mic.0.001586 (2025).
48 Johnson, J. R., Moseley, S. L., Roberts, P. L. & Stamm, W. E. Aerobactin and other virulence factor genes among strains of *Escherichia coli* causing urosepsis: association with patient characteristics. *Infect Immun* **56**, 405-412, doi:10.1128/iai.56.2.405-412.1988 (1988).
49 Johnson, J. R. *et al.* Distribution and characteristics of *Escherichia coli* clonal group A. *Emerg Infect Dis* **11**, 141-145, doi:10.3201/eid1101.040418 (2005).
50 Manges, A. R., Tabor, H., Tellis, P., Vincent, C. & Tellier, P. P. Endemic and epidemic lineages of *Escherichia coli* that cause urinary tract infections. *Emerg Infect Dis* **14**, 1575-1583, doi:10.3201/eid1410.080102 (2008).
51 Guyomard-Rabenirina, S. *et al.* Temporal trends and risks factors for antimicrobial resistant Enterobacteriaceae urinary isolates from outpatients in Guadeloupe. *BMC Microbiol* **16**, 121, doi:10.1186/s12866-016-0749-9 (2016).
52 Sandekian, V. & Lemay, G. A single amino acid substitution in the mRNA capping enzyme lambda2 of a mammalian orthoreovirus mutant increases interferon sensitivity. *Virology* **483**, 229-235, doi:10.1016/j.virol.2015.04.020 (2015).
53 Danis, C. & Lemay, G. Protein synthesis in different cell lines infected with orthoreovirus serotype 3: inhibition of host-cell protein synthesis correlates with accelerated viral multiplication and cell killing. *Biochem Cell Biol* **71**, 81-85, doi:10.1139/o93-012 (1993).
54 Coombs, K. M. Mammalian Reoviruses: Propagation, Quantification, and Storage. *Curr Protoc* **3**, e716, doi:10.1002/cpz1.716 (2023).
55 Georgi, A., Mottola-Hartshorn, C., Warner, A., Fields, B. & Chen, L. B. Detection of individual fluorescently labeled reovirions in living cells. *Proc Natl Acad Sci U S A* **87**, 6579-6583, doi:10.1073/pnas.87.17.6579 (1990).
56 Lanoie, D. & Lemay, G. Multiple proteins differing between laboratory stocks of mammalian orthoreoviruses affect both virus sensitivity to interferon and induction of interferon production during infection. *Virus Res* **247**, 40-46, doi:10.1016/j.virusres.2018.01.009 (2018).
57 Desloges, I. *et al.* Identification and characterization of OmpT-like proteases in uropathogenic *Escherichia coli* clinical isolates. *Microbiologyopen* **8**, e915, doi:10.1002/mbo3.915 (2019).

58 Johnson, J. R. *et al.* Molecular epidemiological and phylogenetic associations of two novel putative virulence genes, iha and iroN (*E. coli*), among *Escherichia coli* isolates from patients with urosepsis. *Infect Immun* **68**, 3040-3047, doi:10.1128/IAI.68.5.3040-3047.2000 (2000).

Table 1. Table of Strains

Catalog #	Name	Species	Characteristic*	Source (ref)
E. coli				
DEF1746	AR3110	*Escherichia coli*	K-12	[39]
QT5740	CFT073	*Escherichia coli*	WT UPEC	C.M. Dozois [40]
QT3511	UTI 1	*Escherichia coli*	UPEC Cystitis 1	H. Le Moual [57]
QT3512	UTI 2	*Escherichia coli*	UPEC Cystitis 2	H. Le Moual [57]
QT3513	UTI 3	*Escherichia coli*	UPEC Cystitis 3	H. Le Moual [57]
QT5518	JAD-1	*Escherichia coli*	Cystitis	C.M. Dozois
QT235	Pyelo76	*Escherichia coli*	Clinical strain	J. Johnson
QT236	JJ717	*Escherichia coli*	Clinical strain	J. Johnson
QT238	2H17	*Escherichia coli*	Clinical strain (B1)	J. Johnson [58]
QT247	U247	*Escherichia coli*	Clonal group A isolate	C. M. Dozois
QT250	V10	*Escherichia coli*	Clinical strain (Puti250)	J. Johnson [58]
QT253	V11	*Escherichia coli*	Clinical strain (JJ718)	J. Johnson [58]
QT256	Fex513	*Escherichia coli*	Clinical strain (Pyelo198)	J. Johnson
QT259	JJ719	*Escherichia coli*	Clinical strain (Pyelo197)	J. Johnson
QT262	JJ721	*Escherichia coli*	Clinical strain (Pyelo73)	J. Johnson
Systemic				
DEF2057	1	*Staphylococcus epidermidis*	PICC	C. Quach
DEF2058	2	*Klebsiella oxytoca*	PICC	C. Quach
DEF2059	3	*Escherichia coli*	PICC	C. Quach
DEF2060	4	*Enterococcus faecalis*	CVC	C. Quach
DEF2061	5	*Klebsiella pneumoniae*	CCVP	C. Quach
DEF2062	6	*Staphylococcus aureus*	PICC	C. Quach
DEF2063	7b	*Staphylococcus epidermidis*	PICC	C. Quach

DEF2064	8b	*Staphylococcus aureus*	PAC	C. Quach
DEF2065	9	*Staphylococcus capitis*	PICC	C. Quach
DEF2066	10b	*Staphylococcus aureus*	PAC	C. Quach
DEF2067	11b	*Staphylococcus epidermidis*	PICC	C. Quach
DEF2068	12	*Klebsiella oxytoca*	PICC	C. Quach
DEF2069	13b	*Staphylococcus aureus*	PICC	C. Quach
DEF2070	14	*Staphylococcus epidermidis*	PICC	C. Quach
DEF2071	15b	*Staphylococcus aureus*	PICC	C. Quach
DEF2072	16b	*Staphylococcus aureus*	PICC	C. Quach
DEF2073	17b	*Enterococcus faecalis*	PICC	C. Quach
DEF2074	18	*Staphylococcus aureus,* SARM	PICC	C. Quach
DEF2075	19	*Staphylococcus epidermidis*	PICC	C. Quach
DEF2076	20	*Staphylococcus epidermidis*	CVC	C. Quach
DEF2077	21	*Staphylococcus epidermidis*	PICC	C. Quach
DEF2078	22	*Staphylococcus epidermidis*	CVC	C. Quach

*

PICC: Peripherally-inserted central catheter.

CVC: Central venous catheter

CVCP : Central venous catheter port

PAC: port-a-catheter/implantable port

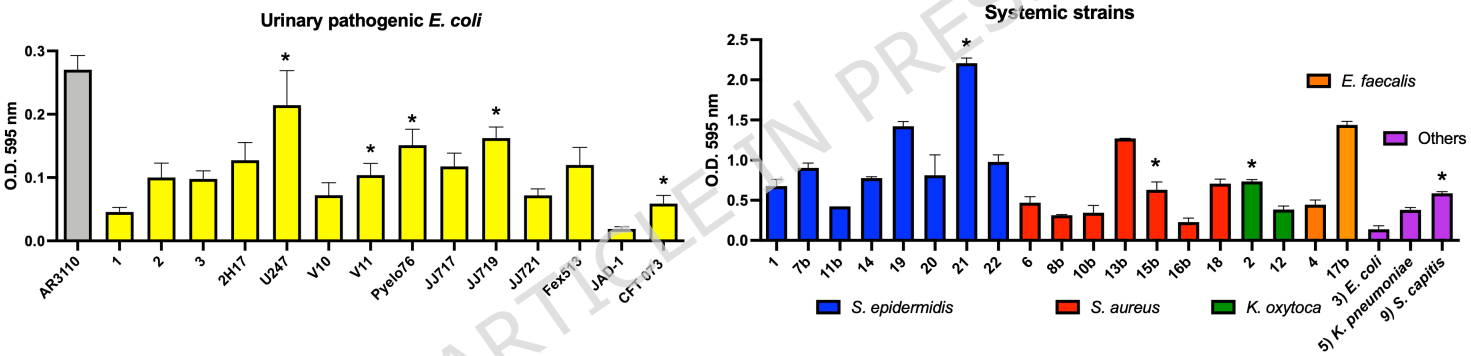

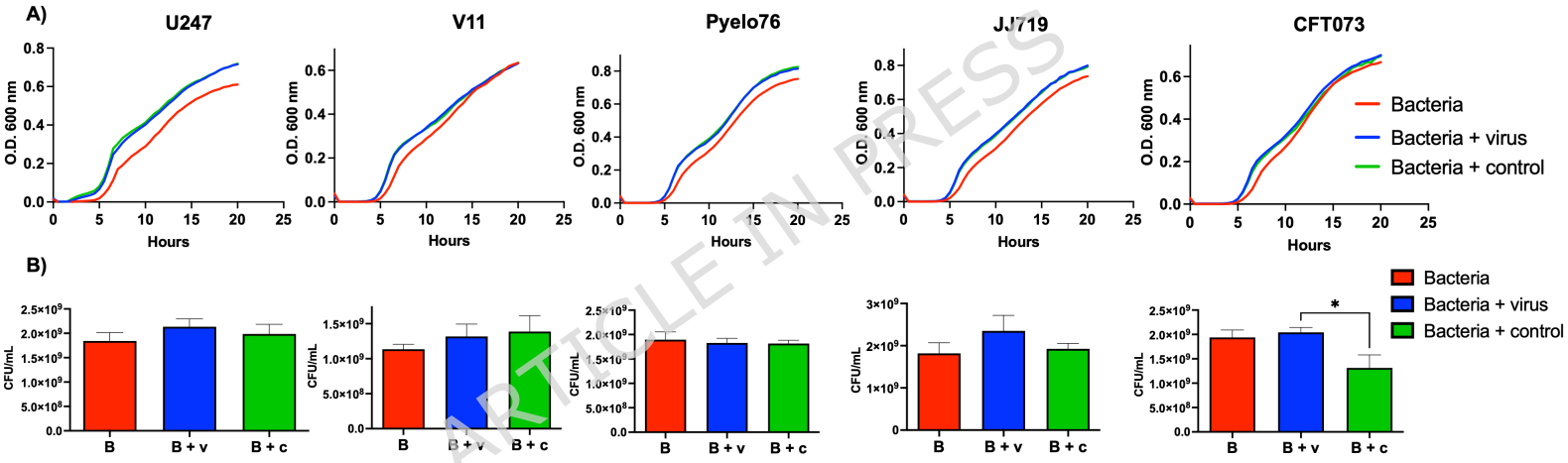

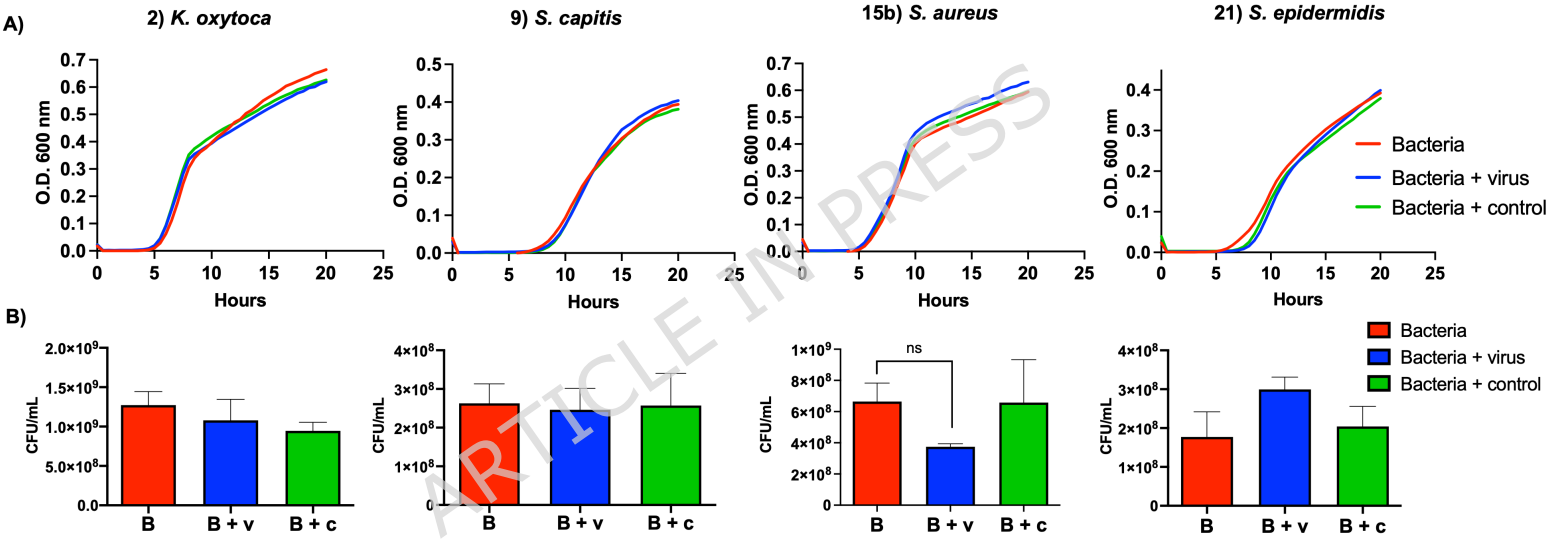

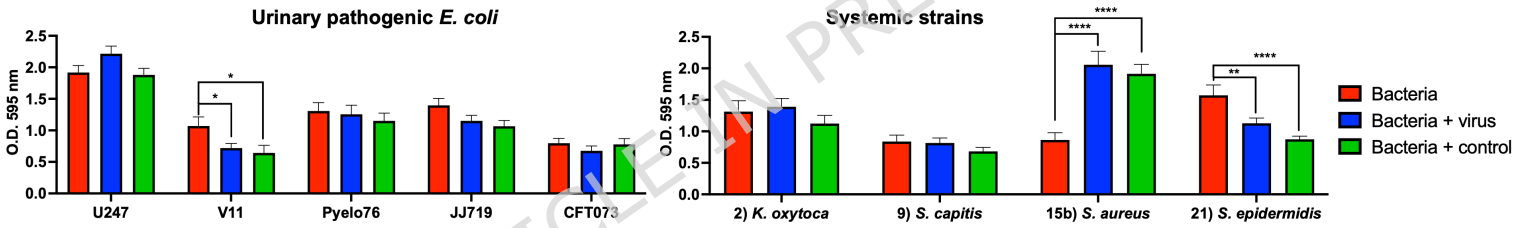

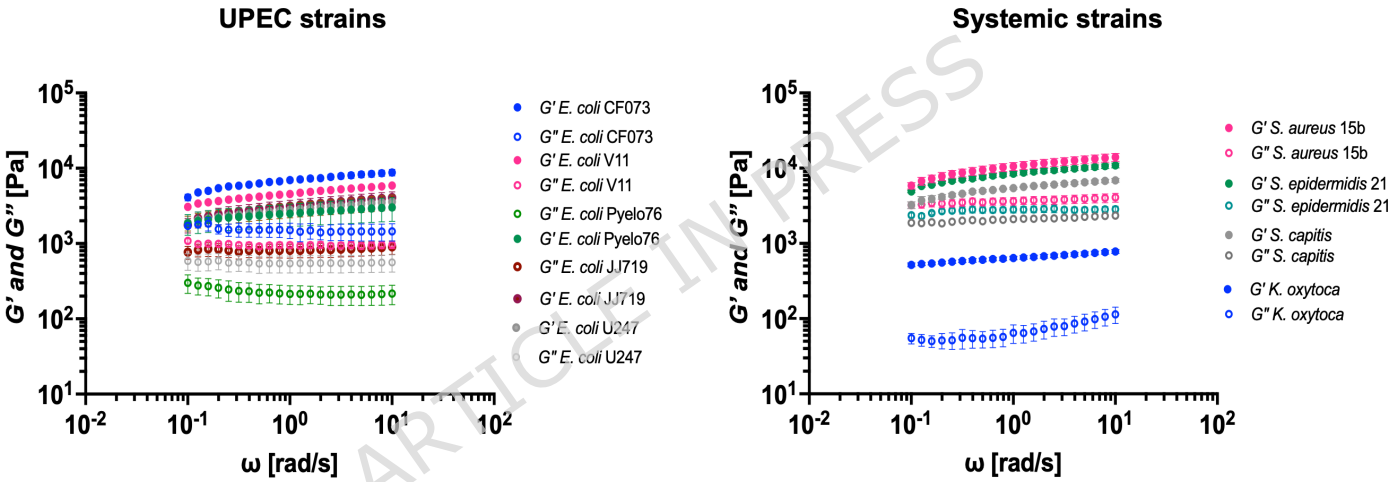

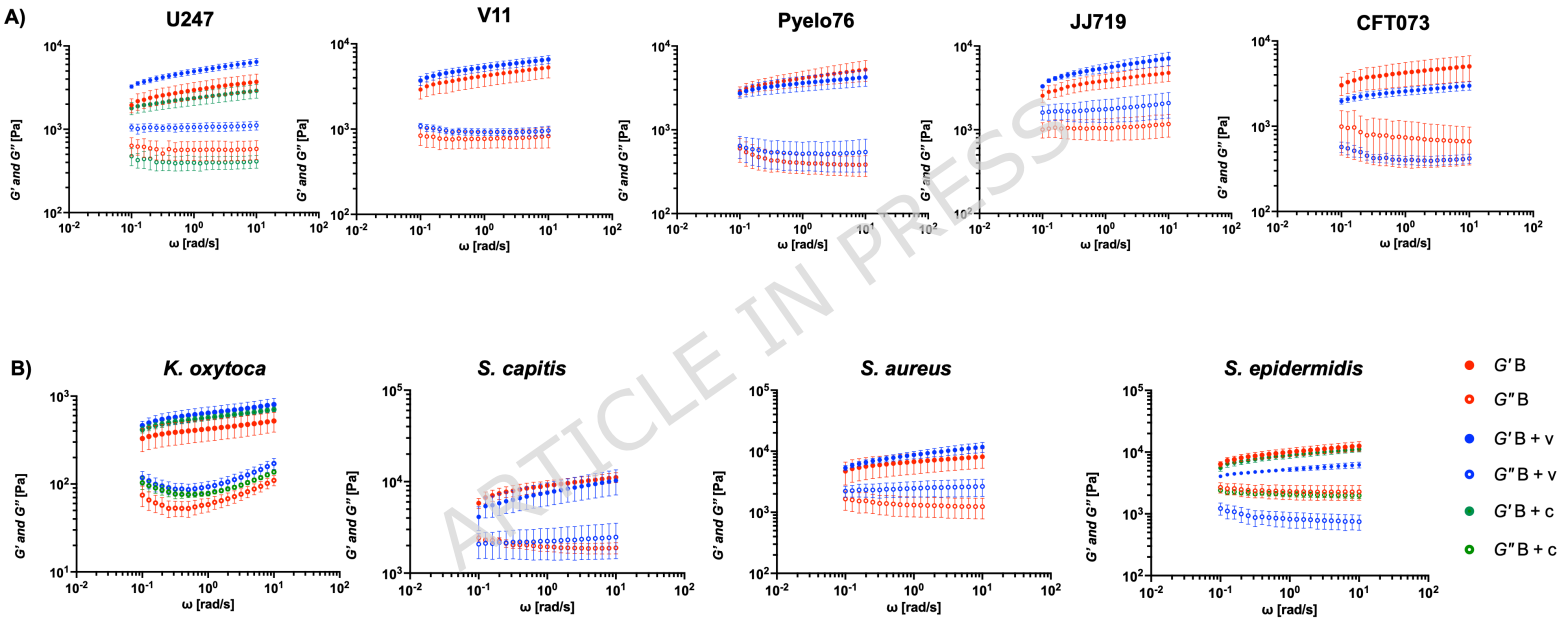

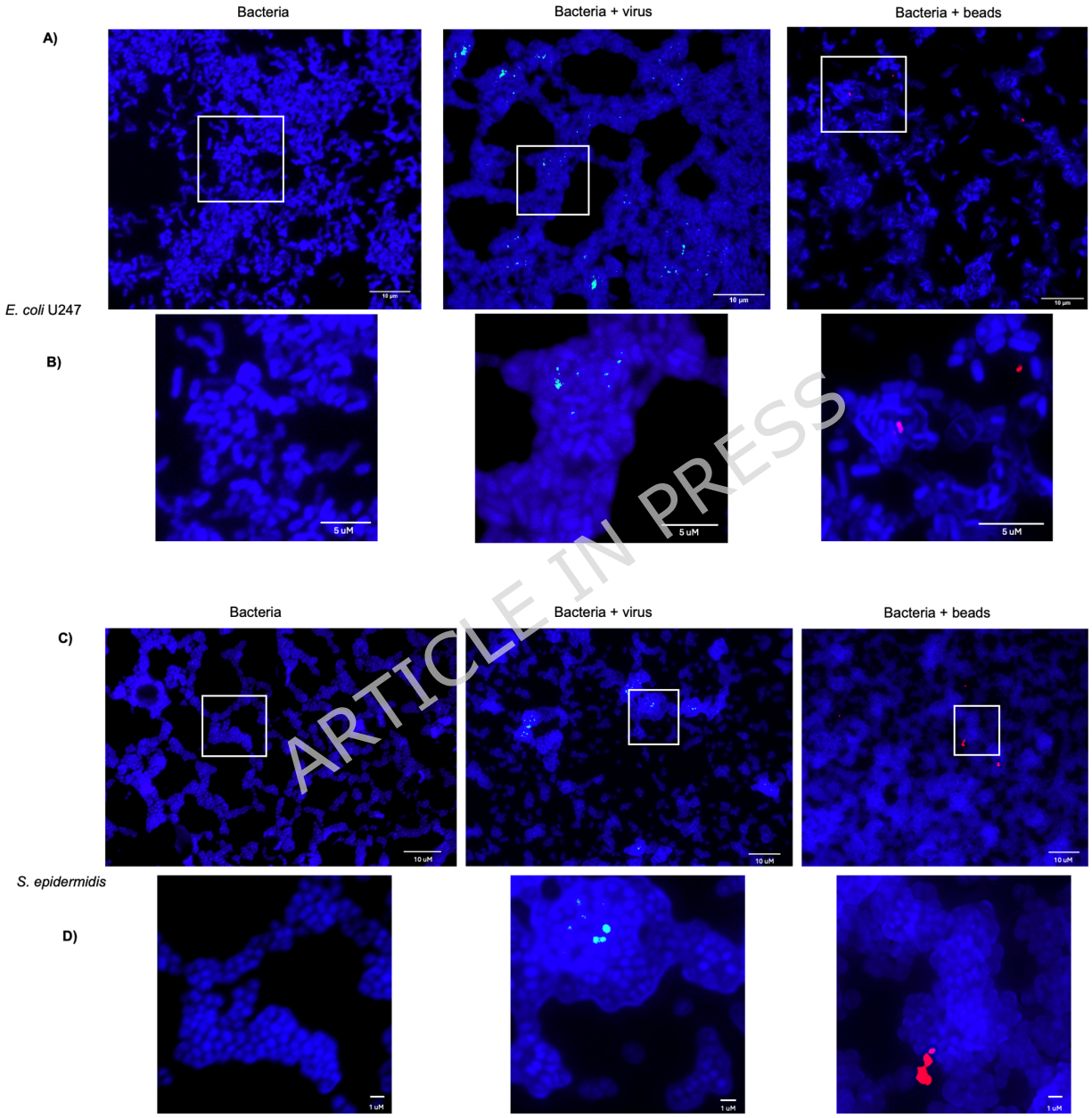

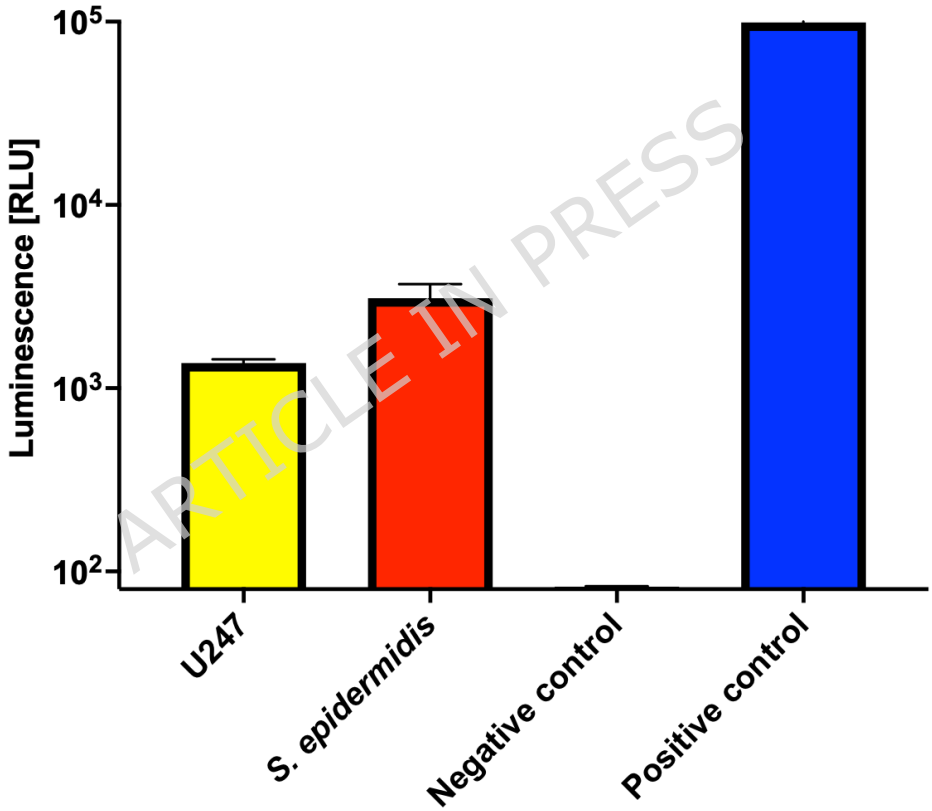

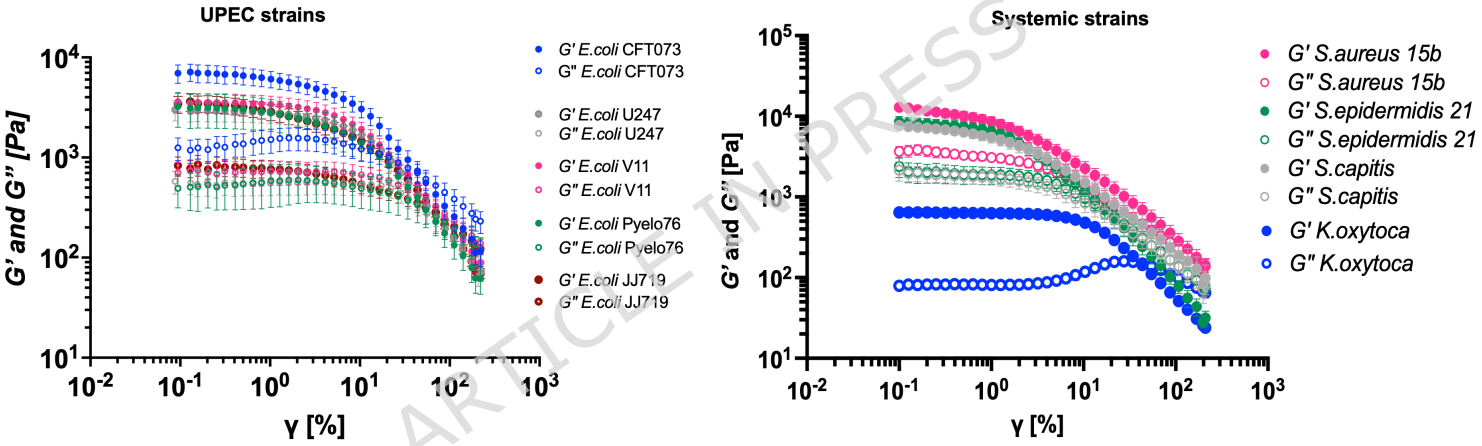

Table 1. Table of Strains

Catalog #	Name	Species	Characteristic*	Source (ref)
E. coli				
DEF1746	AR3110	*Escherichia coli*	K-12	[28]
QT5740	CFT073	*Escherichia coli*	WT UPEC	C.M. Dozois [29]
QT3511	UTI 1	*Escherichia coli*	UPEC Cystitis 1	H. Le Moual [46]
QT3512	UTI 2	*Escherichia coli*	UPEC Cystitis 2	H. Le Moual [46]
QT3513	UTI 3	*Escherichia coli*	UPEC Cystitis 3	H. Le Moual [46]
QT5518	JAD-1	*Escherichia coli*	Cystitis	C.M. Dozois
QT235	Pyelo76	*Escherichia coli*	Clinical strain	J. Johnson
QT236	JJ717	*Escherichia coli*	Clinical strain	J. Johnson
QT238	2H17	*Escherichia coli*	Clinical strain (B1)	J. Johnson [47]
QT247	U247	*Escherichia coli*	Clonal group A isolate	C. M. Dozois
QT250	V10	*Escherichia coli*	Clinical strain (Puti250)	J. Johnson [47]
QT253	V11	*Escherichia coli*	Clinical strain (JJ718)	J. Johnson [47]
QT256	Fex513	*Escherichia coli*	Clinical strain (Pyelo198)	J. Johnson
QT259	JJ719	*Escherichia coli*	Clinical strain (Pyelo197)	J. Johnson
QT262	JJ721	*Escherichia coli*	Clinical strain (Pyelo73)	J. Johnson
Systemic				
DEF2057	1	*Staphylococcus epidermidis*	PICC	C. Quach
DEF2058	2	*Klebsiella oxytoca*	PICC	C. Quach
DEF2059	3	*Escherichia coli*	PICC	C. Quach
DEF2060	4	*Enterococcus faecalis*	CVC	C. Quach
DEF2061	5	*Klebsiella pneumoniae*	CCVP	C. Quach
DEF2062	6	*Staphylococcus aureus*	PICC	C. Quach
DEF2063	7b	*Staphylococcus epidermidis*	PICC	C. Quach
DEF2064	8b	*Staphylococcus aureus*	PAC	C. Quach

DEF2065	9	*Staphylococcus capitis*	PICC	C. Quach
DEF2066	10b	*Staphylococcus aureus*	PAC	C. Quach
DEF2067	11b	*Staphylococcus epidermidis*	PICC	C. Quach
DEF2068	12	*Klebsiella oxytoca*	PICC	C. Quach
DEF2069	13b	*Staphylococcus aureus*	PICC	C. Quach
DEF2070	14	*Staphylococcus epidermidis*	PICC	C. Quach
DEF2071	15b	*Staphylococcus aureus*	PICC	C. Quach
DEF2072	16b	*Staphylococcus aureus*	PICC	C. Quach
DEF2073	17b	*Enterococcus faecalis*	PICC	C. Quach
DEF2074	18	*Staphylococcus aureus,* SARM	PICC	C. Quach
DEF2075	19	*Staphylococcus epidermidis*	PICC	C. Quach
DEF2076	20	*Staphylococcus epidermidis*	CVC	C. Quach
DEF2077	21	*Staphylococcus epidermidis*	PICC	C. Quach
DEF2078	22	*Staphylococcus epidermidis*	CVC	C. Quach

*

PICC: Peripherally-inserted central catheter.

CVC: Central venous catheter

CVCP : Central venous catheter port

PAC: port-a-catheter/implantable port